Proceedings IRG Annual Meeting (ISSN 2000-8953)

IRG/WP 14-30653

THE INTERNATIONAL RESEARCH GROUP ON WOOD PROTECTION

Section 3 **Wood protecting chemicals**

Visualization of gold/silver nanostars in wood by surface enhanced Raman spectroscopy

C. Geers[1], L. Rodríguez-Lorenzo[1], MI. Placencia Peña[2], P. Brodard[3], T. Volkmer[2], B. Rothen-Rutishauser[1], A. Petri-Fink[1]

[1]Adolphe Merkle Institute – University of Fribourg
Bionanomaterials Group
Rte de l'Ancienne Papeterie CP 209
1723 Marly, Switzerland

[2]Berner Fachhochschule – Architektur, Holz und Bau
Solothurnstrasse 102
2500 Biel, Switzerland

[3]College of Engineering and Architecture of Fribourg
Pérolles 80
1705 Fribourg, Switzerland

Paper prepared for the 45th IRG Annual Meeting
St George, Utah, USA
11-15 May 2014

IRG SECRETARIAT
Box 5609
SE-114 86 Stockholm
Sweden
www.irg-wp.com

Visualization of gold/silver nanostars in wood by surface enhanced Raman spectroscopy

C. Geers[1], L. Rodríguez-Lorenzo[1], MI. Placencia Peña2, P. Brodard[3], T. Volkmer[2], B. Rothen-Rutishauser[1], A. Petri-Fink[1]

[1]Adolphe Merkle Institute, University of Fribourg,
Route de l'Ancienne Papeterie CP 209, 1723 Marly, Switzerland
e-mail: christoph.geers@unifr.ch; alke.fink@unifr.ch

[2]Bern University of Applied Sciences – Architecture, Wood and Civil Engineering
Solothurnstrasse 102, 2500 Biel, Switzerland

[3]College of Engineering and Architecture of Fribourg,
Pérolles 80, CH-1705 Fribourg, Switzerland

ABSTRACT

Nanotechnology is a fast growing up-to-date technology and ventures expeditiously in the wood preservative market. However, there is still a huge lack of understanding about the interaction and incorporation of nanoparticles (NSs) in wood. Surface-enhanced Raman scattering (SERS) offers unique advantages as an analytical tool with a high selectivity and sensitivity without matrix interference. Here, we design and fabricate SERS-tagged silver/gold nanostars (NSs), coated with a silica shell encapsulating nile blue A (NBA), as potential platforms for SERS imaging. These NSs can be pressure-impregnated in different wood types (pine and beech) due their optimal size (< 100 nm), allowing for their rapid and accurate identification and localization in the wood samples. For comparison and visualization of the NSs, the samples were coated with a carbon layer for analysis in a scanning electron microscope (SEM). We demonstrate that SERS provides advantages over SEM. The NSs can be visualised by SERS without coating of the samples. In addition, no vacuum is needed to image the NSs, and the excitation laser line (633 nm) used applies a lower energy for detection of NSs than the electron beam of the SEM. These facts lead to a much decreased formation of artefacts during NSs detection in wood. This quick and easy method can be used for fast analysis of new nanoparticle-based wood preservative systems, which leads to a better understanding of impregnation processes, providing an essential step in finding fundamentally new wood preservatives.

Keywords: nanoparticle, wood preservative, impregnation, SERS

1. INTRODUCTION

The wood preservation industry is one of the largest markets for the application of nanotechnology (Leach 2005). Although this technology is still in the early stages of development, its enormous potential has already been recognized (Evans *et al.* 2008). It is well accepted that nanotechnology might help improve existing materials or develop entirely new, more efficient or cheaper wood preservatives. However, evaluating the potential of nanomaterials requires more fundamental studies about the materials (e.g. their size distribution and colloidal stability), the impregnation process, particle localization, as well as leaching and biocidal efficiency trials (Kamel 2007, Evans *et al.* 2008). For example, micronized copper formulations containing copper (nano)particles, are used in large-scale to treat lumber for ground contact use (Leach 2005).

However, formulation, impregnation processes and mode of action are not yet fully understood, which indicates that plenty of research is still necessary in this recent application of nanotechnology (Freeman and McIntyre 2008, Evans *et al.* 2008). At present, the implementation is comparable to other fields, where nanotechnology is likely to have a huge impact on future applications, such as medicine or food technology (Jones 2008) and would profit from much closer collaboration between the fields (Evans *et al.* 2008).

One basic requirement to study aggregation, localization, mode of action, and fate of impregnated nanoparticles (NPs) is their visualization in the wood structure. However, conventional methods for detection often require substantial sample preparation. For electron microscopy, specimens are usually required to be dry. Several methods can be used to dry samples but the risk of inducing artefacts during this drying process is relatively high (Gilkey and Staehelin 1986). In addition, transmission electron microscopy (TEM) can achieve a point resolution in nanometer range but requires epoxy embedded and ultrathin sectioned (50-100 nm) samples (Maurer and Fengel 1991). Compared to TEM, scanning electron microscopy (SEM) allows studying the surface of larger objects but relies on sample coatings (e.g. with carbon, platinum or gold) to ensure electron conductivity of the material (Mukhopadhyay 2003). Optical microscopy techniques do not require sample preparation but lack the resolving power, limited to about 200 nm, to detect single NPs in the wood structure.

Usually, fluorescence microscopy techniques are the most widely used for NP characterization in different complex matrices, such as biological and polymeric samples (Michalet *et al.* 2005, Amin *et al.* 2012, Fenniri and Álvarez-Puebla 2007). The technique generally offers a high degree of sensitivity, down to single-molecule detection levels (Kozak *et al.* 2011, Weiss 1999). In fact, fluorescence microscopy has been successfully applied to visualize the relative amount of lignin, an auto-fluorescent polymer, amongst different wood cells (Ma *et al.* 2013). However, the detection of single (nano)particles is limited by the spatial resolution of the optical microscope (> 200 nm).

Surface-enhanced Raman scattering (SERS) might be an alternative imaging technique. It can provide high throughput chemical information on particles with sizes down to the nanometre scale. SERS is based on the enhancement of the Raman signal up to 10^{10} for molecules adsorbed on a metal NP surface (Fleischmann *et al.* 1974, Kneipp *et al.* 1997). This enhancement is principally caused by the excitation of the collective oscillations of the conduction electrons in a metal NP, the so-called localized surface plasmon resonance (LSPR). Excitation of the LSPR results in the enhancement of the local field experienced by a molecule adsorbed on the NP surface (Jeanmaire and van Duyne 1977, Albrecht and Creighton 1977). In addition, the SERS spectrum is a unique signature containing all the vibrational information of the adsorbed molecule (Álvarez-Puebla 2012), and the measurement can be carried out under various conditions without any sample preparation.

Concerning particle structure, 2 approaches are feasible in SERS imaging: Metal NPs can be used as optical sensors, allowing the characterization of the components in the sample. Based on this, Agarwal & Reiner (Agarwal and Reiner 2009) recorded the SERS spectrum of lignin using silver NPs, demonstrating the incredible capacity of SERS to characterize wood samples. Using SERS tags, i.e. metal NPs plus a reporter (e.g. a dye) molecule, an extremely strong signal can be obtained, which decreases both the amount of NPs necessary to acquire the relevant information and the time for the read-out (Álvarez-Puebla and Liz-Marzán 2010). Therefore, NPs are coated with a protective mono- or multi-layer (e.g. silica, polyelectrolytes). The shell in these coated particles, known as encoded particles, protects the NPs e.g. against oxidation, limits aggregation, provides the possibility of subsequent surface functionalization, and can confer biocompatibility

(Doering and Nie 2003, Doering *et al.* 2007, Fernández-López *et al.* 2009). As such, an ideal SERS substrate for wood imaging applications should induce a high signal enhancement, generate a reproducible and uniform response, have a long shelf life, and should be easy to synthesize (Qian and Nie 2008). Gold nanostars (AuNSs) are promising candidates, since they show a large local electromagnetic field enhancement at the apex of their tips. (Hao *et al.* 2007) Those locally enhanced fields have been exploited to amplify Raman signals allowing molecular detection at the zeptomol regime (Rodríguez-Lorenzo *et al.* 2009) and have even enabled the demonstration of SERS from a single molecule adsorbed to a single nanoparticle (Hrelescu *et al.* 2009). Moreover, the optical and spectroscopic properties of AuNSs can be tuned by simple coating and surface functionalization techniques (Rodríguez-Lorenzo *et al.* 2012, Rodríguez-Lorenzo *et al.* 2011a, Rodríguez-Lorenzo *et al.* 2011b).

In this manuscript, Nile Blue A/SERS-tagged silica coated gold/silver nanostars (Au/AgNSs) are investigated as a potential platform to study the potential of newly develop NPs for wood preservation with minimal sample preparation. SERS imaging is compared to SEM-EDX mapping and it is shown that the impregnation of wood with engineered NSs can be exploited for the rapid and ultra-sensitive SERS-based visualisation in wood samples at the nano scale.

2. Experimental Methods

2.1 Wood

Wood species used were beech (*Fagus sylvatica*) and pine (*Pinus sylvestris*) and all samples were selected according to EN113. The wood samples were cut into pieces of 50x25x15 mm^3 for impregnation. Control by gravimetric analysis after impregnation was omitted as it is not applicable for nanoparticle impregnated wood.

2.2 Synthesis of silver/gold nanostars (Au/AgNSs)

Gold nanostars (AuNSs) were prepared by adding poly(vinylpyrrolidone) (PVP)-coated gold seeds ([Au] = 5 x 10^{-5} M; d=15 nm) in ethanol to a mixture of $HAuCl_4$ (0.5 mM) and PVP (M_w = 10 000, 10 mM) in N,N-dimethylformamide (DMF) under rapid stirring at room temperature. The as-prepared AuNSs dispersion was purified, concentrated by centrifugation (3500 rpm, 60 min), and the pellets were redispersed in ethanol. The final gold concentration was estimated from the absorbance at 400 nm (Cardinal *et al.* 2014).

The silver deposition step was achieved by adding 100 µL of 10 mM of PVP solution and 100 µL of H_2O_2 (30% v/v) to the AuNSs ([Au] = 0.5 mM) in water. Subsequently, $AgNO_3$ (0.14 mM) and NH_3 (4 mM) were added to trigger the reduction of silver ions on the AuNSs. Spectral changes were measured with a Jasco V-670 UV-Vis-NIR spectrophotometer after 24 h of reaction.

2.3 Encoding and silica coating of Au/AgNSs (AuAg NSs@NBA@SiO_2)

To prepare silica coated-Au/AgNSs with an embedded Raman reporter, particles were centrifuged (2500 rpm, 30 min) and redispersed in ethanol to a final gold concentration of 0.5 mM. Then, nile blue A (NBA) was added under rapid stirring to a concentration not exceeding 6 µM and was allowed to equilibrate for 10 min. Finally, a silica coating was applied following the procedure of Kobayashi *et al.* 2005 using the following concentrations: [H_2O] = 10.55 M, [dimethylamine (DMA)] = 0.06 M, and [tetraethylorthosilicate (TEOS)] = 2 mM. The reaction mixture was allowed to react for 24 h and the final particles were centrifuged (2000 rpm, 30 min) and washed with water.

2.4 Characterization

Optical characterization was carried out by UV-Vis-NIR spectroscopy with a Jasco V-670 spectrophotometer, using 10 mm path length quartz cuvettes. A Hitachi transmission electron microscope (TEM) operating at an acceleration voltage of 80 kV was used for particle size analysis (Image J). The Au/AgNSs@NBA@SiO_2 dispersion was spin-coated on a standard holey carbon film supported by a TEM grid.

2.5 Impregnation

The dry wood samples were incubated in the NSs suspension in plastic flasks and placed in an autoclave for timber treatment. First a vacuum of -95 mbar was applied for 20 min, followed by a pressure of 5 bars for 1 h. The wood samples were entirely submerged in the NSs suspension using a plastic grid. After impregnation the wood samples were dried at room temperature for at least 48 h.

2.6 Surface-enhanced Raman scattering

Dried wood samples were carefully split in radial direction using a scalpel. The exposed wood surface was analysed upon excitation with a 633 nm laser line, using a Lab Ram HR microRaman system from Horiba-Jobin Yvon equipped with a confocal optical microscope, high resolution grating (1800 g/mm) and a Peltier-cooled CCD detector. SERS mapping was carried out in areas of 52 × 36 μm^2, with a step size of 2.5 μm, with accumulation times of 50 s and laser power at the sample of 350 μW. The laser was focused onto the sample by using a 100× objective (N.A. 0.9) providing a spatial resolution of 1 μm.

2.7 Scanning electron microscopy

After SERS analysis the split wood sample was glued to a graphite plate using conductive carbon paste. The exposed wood surface was coated with a 30 nm layer of carbon to ensure conductivity. The samples were analysed on a FEI XL30 Sirion FEG scanning electron microscope using a secondary electron (SE) detector and for high resolution images a through the lens (TLD) detector at a voltage of 3 kV and 5 mm working distance.
The samples were mapped using an energy dispersive x-ray spectrometer from EDAX equipped with lithium doped silicon detector and analysed using EDAX Genesis software version 5.2.

3. RESULTS AND DISCUSSION

Figure 1A-C show representative TEM images of different stages in the synthesis of the silica-coated Au/AgNSs used for wood impregnation and as a platform for SERS imaging. The synthesis of AuNSs was based on a previously reported method (Kumar *et al.* 2007), involving the reduction of $HAuCl_4$ in a concentrated solution of PVP in DMF in presence of pre-synthesized AuNP seeds (Figure 1A). It has been shown before that PVP kinetically controls the reduction of $AuCl_4^-$ on the Au seeds, which results in the formation of AuNSs (Kumar *et al.* 2007). The obtained AuNSs were used as new seeds for subsequent Ag growth by H_2O_2 mediated reduction of $Ag(NH_3)_2^+$ (Chen *et al.* 2009). Interestingly, the Ag-coated Au core (45 ± 11 nm in diameter) preserves the star-like morphology (Figure 1B), which is beneficial for SERS due to the large electromagnetic field concentration localized at the tips, as previously demonstrated by electron energy loss spectroscopy (EELs) mapping and theoretical modelling (Rodríguez-Lorenzo *et al.* 2009). The silver coating is applied as silver provides an additional enhancement; it gives rise to a 10- to 100 fold increased SERS signal compared to AuNPs (de Abajo 2007). Subsequent silica coating was performed using a modified Stöber method (Stöber *et al.* 1968). Dimethylamine was selected as the alkaline catalyst rather than ammonia (Kobayashi *et al.* 2005) to avoid reshaping during the silica coating process. In this kind of hybrid composite, the Au/Ag core provides a high electromagnetic field, which is necessary for the enhancement of the Raman signal of given SERS reporters. The silica coating (i) protects the

Raman tag from leaching, (ii) inhibits the adsorption of other molecules on the metal surfaces, which might interfere with the vibrational fingerprint, (iii) hampers silver oxidation, and (iv) increases colloidal stability of the suspension. Encapsulation of NBA was achieved by the addition of the dye to the PVP-stabilized Au/AgNSs prior to the reaction with TEOS. The cationic nature of NBA (Figure 1) is likely to trigger adsorption on the negatively charged Au/AgNS surface during silica coating. This was confirmed by TEM, which shows that each individual Au/AgNS was coated with a thin, uniform silica shell of around 15 nm (Figure 1C). Figure 1D shows the evolution of the VIS-NIR spectra during the synthetic procedure. AuNSs present the typical two LSPR modes corresponding to the field localization at the central core and the tips (Kumar *et al.* 2007, Rodríguez-Lorenzo *et al.* 2009). The initially prepared AuNSs display a well-defined LSPR band centred at 794 nm (tip mode) and a weaker shoulder at 560 nm corresponding to the core mode. The growth of the silver shell on AuNSs results in a blue-shift of 85 nm in the LSPR of the Au NSs due to the hybridization of the dielectric constants of gold and silver (Prodan *et al.* 2003). Notably, the position of the tip plasmon mode is now in better resonance coupling with the excitation laser lane (633 nm) used for SERS experiments, which will provide higher enhancement as has been demonstrated in typical surface-enhanced Raman excitation spectroscopy (SERES) experiments (Zhao *et al.* 2008, Etchegoin *et al.* 2006). As previously reported, (Liz-Marzán *et al.* 1996) coating metal NPs with silica gives rise to a significant red shift of 10 nm in the corresponding LSPR bands as displayed in the VIS-NIR spectrum plotted in Figure 1B. This effect can be explained with the higher refractive index of amorphous silica (1.46) compared to ethanol (1.36), which produces a decrease in the restoring force on the electron oscillation associated with the plasmon modes (Mulvaney 1995).

The optical-enhancing properties of the Au/AgNSs@NBA@SiO_2 are demonstrated in Figure 1F, where the vibrational spectrum of NBA is shown. It is important to mention that aqueous NBA has an electronic absorption band centred at 627 nm (Figure 1E), which is close to the excitation wavelength of the excitation laser line used for the SERS measurements (633 nm). Therefore, the spectrum has contributions to the enhanced local field from LSPRs of Au/AgNSs and the resonance Raman effect, and it is more precisely described as surface-enhanced resonance Raman scattering (SERRS). A 2-3 orders of magnitude higher sensitivity is expected due to this electronic resonance (Aroca 2007). Moreover, in order to demonstrate the benefits of the silver coating for SERRS detection, the intensity of the signals of NBA provided by the regular silica-coated Au NSs and Au/AgNSs@NBA@SiO_2 was compared. The signal acquired from the substrate clearly showed the characteristic vibrational pattern of NBA (Álvarez-Puebla *et al.* 2009): ring stretching (1643, 1492, 1440, 1387, 1351, and 1325 cm^{-1}), CH bending (1258, 1185 cm^{-1}), and the in-plane CCC and NCC (673 cm^{-1}), CCC and CNC (595 cm^{-1}), and CCC (499 cm^{-1}) deformations. Given the demonstrated efficiency of AuNSs for ultrasensitive SERRS (Rodríguez-Lorenzo *et al.* 2014), it was all the more remarkable that the intensity of the spectra obtained with Au/AgNSs@NBA@SiO_2 was 4-fold higher when compared to that of the "bare" AuNSs coated with silica.

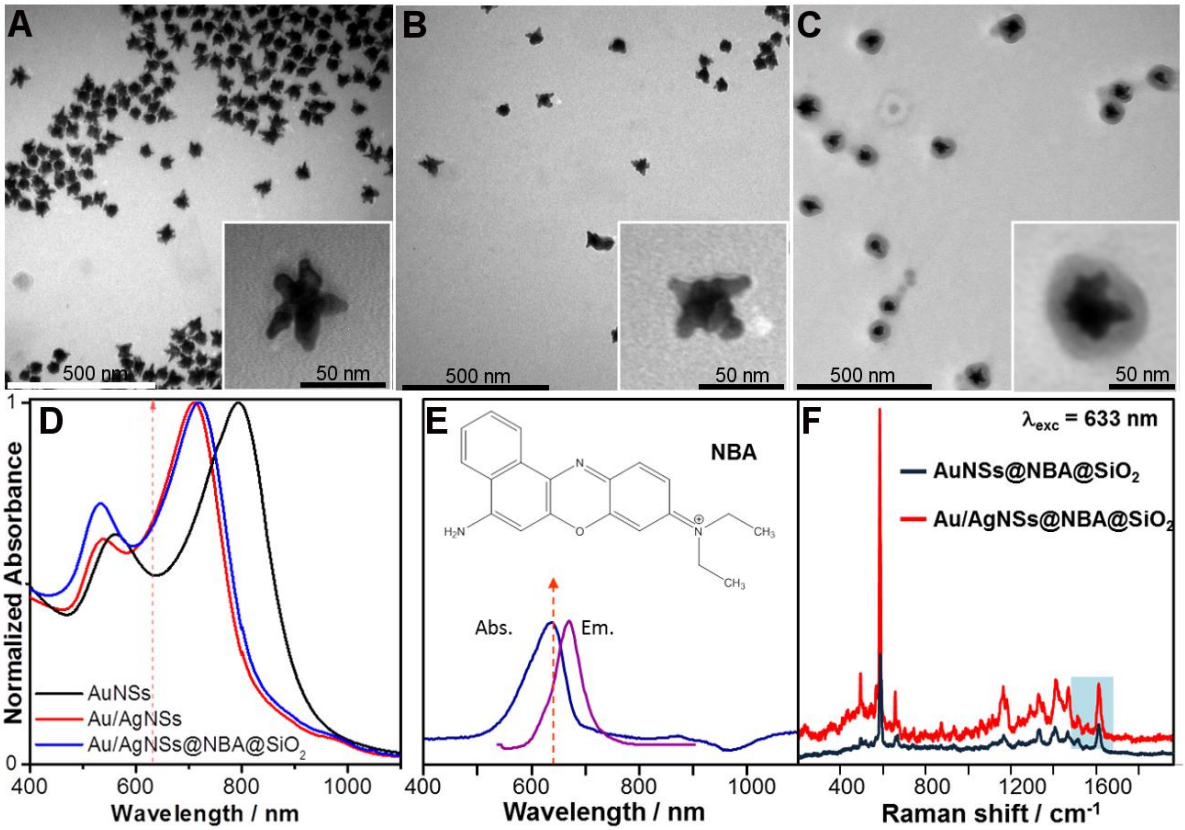

Figure 1. TEM images of AuNSs (A), Au/AgNSs (B) and Au/AgNSs@NBA@SiO2 (C). (D) Localized surface plasmon resonance spectra for NSs, as prepared, after silver reduction and surface modification (i.e. silica coating). The yellow dashed arrow indicates the wavelength of the excitation laser line. (E) Electronic absorption and emission for Nile Blue A (NBA). Both, absorption and emission were recorded in ethanolic solutions (F) SERRS spectrum of the encoded AuNSs and Au/AgNSs upon excitation with a visible 633 nm laser line. The blue marked part was chosen for analysis of the SERRS map (Figure 2).

The fully coated NPs (i.e. Au/AgNSs@NBA@SiO_2) were pressure impregnated in beech (*Fagus sylvatica*) and pine (*Pinus sylvestris*) wood samples at a concentration of 5×10^{13} particles in a final volume of 20 mL. In order to localize the particles inside the wood, samples were studied in a confocal micro-Raman system. During these measurements, SERRS maps were collected in the same spatial region for both wood samples (52×36 μm^2) at the spectral window from 1570 to 1690 cm^{-1} (Figure 2A), to identify one of the characteristic peaks of NBA (1643 cm^{-1}). It should be noted that the bands at 673 and 595 cm^{-1} correspond to the chromophore (phenoxazine), which are significantly more enhanced in SERRS. However, these bands overlap with the auto-fluorescence (Pandey *et al.* 1998) of the wood, which can decrease the detection limit of the method. Moreover, variations in the position and the shape of the 595 cm^{-1} band as well as fluctuations in integrated SERRS intensities in silver nanoshells on polystyrene microspheres have been reported (Izumi *et al.* 2014), increasing the difficulty of data interpretation.

As observed in the control experiments (i.e. wood impregnated with a NP free medium), the applied low excitation intensity and collection time per spectrum did not enable the acquisition of normal Raman spectra from the wood samples (Figure 2A). Interesting, NSs were localized in both wood samples with a remarkable SERRS intensity (Figure 2). In beech wood, the NSs were

detected in vessels and tracheids located close to the vessels (Figure 2B and C), whereas in pine wood, particles were found in axial tracheids and in rays (Figure 2D and E). The SERRS intensity in pine is significantly lower (3-fold) compared to the intensity in beech, as shown in the SERRS spectra in Figure 2A. Differences of the impregnation efficiency were not evaluated, as this study was designed to show the feasibility to use such materials as SERS encoded particles for wood labelling to study nanoparticle interaction and distribution with and in different types of wood.

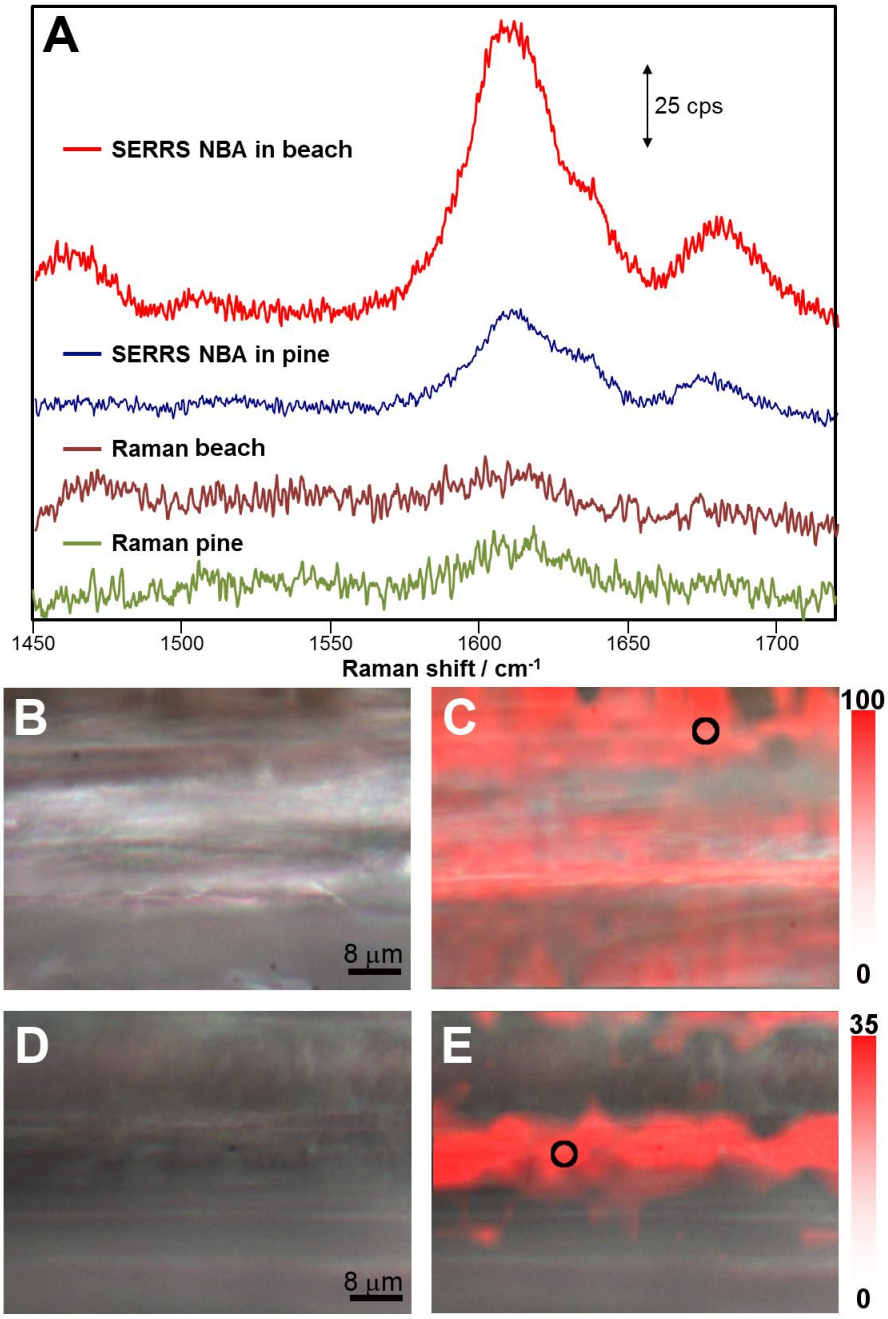

Figure 2. (A) SERRS spectra of NBA in beach and pine and Raman spectra of both wood types. Optical and SERRS images of beech (B, C) and pine (D, E) wood for Au/AgNSs@NBA@SiO2. SERRS map (intensity at 1643 cm^{-1}, 52 × 36 μm^2, stepsize 2.5 µm) was acquired upon excitation with a 633 nm laser line. NSs were localized in both cases with different distribution and particle density as shown in the maps. Black circles show corresponding representative spectra (A).

The presence and localization of encoded NSs were confirmed by SEM. Figure 3 A and B show SEM images of *the same area* of the beech and pine wood samples, which were analyzed by SERRS. The images illustrate the wood structure after splitting, showing some parts were destroyed probably due to the force applied during splitting of the samples, artifacts of the carbon coating (Bråten 1978), or the energy of the electron beam (Egerton *et al.* 2004). Sample preparation severely complicates the examination of NPs in wood by SEM and even in high resolution imaging, NPs are often difficult to detect. An EDX spectral map was recorded to detect the corresponding signals from gold, silver or silica of the NSs. The resolution and settings for the scanning time were adjusted to be comparable to the SERS mapping. No signal of the NSs could be detected in the EDX maps both for pine and beech wood (data not shown). However, SEM at high magnification (Figure 3C) and EDX analysis (Figure 3D) provide clear evidence that Au/AgNSs@NBA@SiO2 can be localized on the cell wall of a beech vessel. In pine wood the NSs could not be differentiated from cell wall structures in SEM images at high magnification (data not shown). These results were consistent with previously reported SERS characterizations of encoded particles in HeLa cells (Rodríguez-Lorenzo *et al.* 2011a), where it was demonstrated that the internalization of a comparatively small number of AuNSs in cells display a higher SERS intensity compared with spherical AuNPs. This optical efficiency is in accordance with the electromagnetic field concentration at the apex of the tips of the NSs (Rodríguez-Lorenzo *et al.* 2009). It should also be noted that after mapping of the samples, no visible signal of damage was observed in the wood, indicating that chosen conditions are adequate for long-time SERS/SERRS experiments.

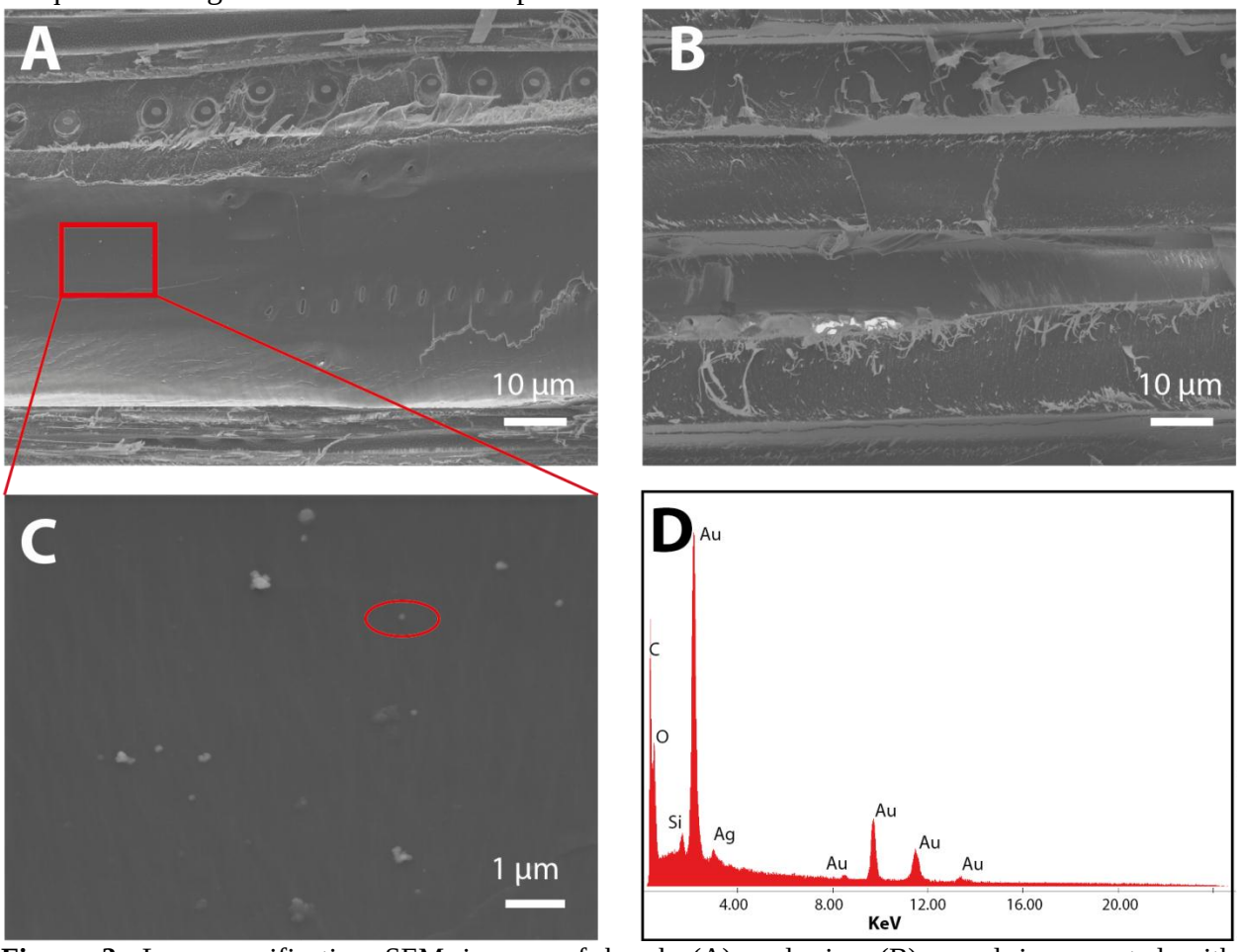

Figure 3. Low-magnification SEM images of beech (A) and pine (B) wood impregnated with Au/AgNSs@NBA@SiO2 (SE, 3kV, WD 5 mm). (C) High-magnification SEM image of the vessel cell wall of beech wood, showing the presence of single Au/AgNSs@NBA@SiO2 and aggregates (TLD, 3kV, WD 5 mm). (D) EDX elemental analysis of Au/AgNSs@NBA@SiO2 from the image in (C).

4. CONCLUSION

This study has clearly demonstrated the great benefit of using encoded and silica-silver coated AuNSs as SERS imaging labels. It could be shown that the impregnation of a few NPs with particular morphology can be exploited for the rapid and ultra-sensitive SERS-based visualisation in wood samples at the nano scale. The encoded NSs were detected by SERS without complex or destructive sample preparation methods compared to electron microscopy at nanometer resolution or EDX analysis. In regards to the development of novel NP-based technologies the here presented method will also be useful to detect biocide molecules and NPs in parallel. Additionally it is conceivable that leaching experiments or quantifications can be performed using the presented detection method.

5. ACKNOWLEDGEMENT

This work was financially supported by the Swiss National Foundation (136976), the Adolphe Merkle Foundation and the University of Fribourg. The Earth Science Unit (University of Fribourg) is acknowledged for the use of the Scanning Electron Microscope.

6. REFERENCES

Agarwal, U P, Reiner, R S (2009): Near-IR surface-enhanced Raman spectrum of lignin. *Journal of Raman Spectroscopy,* **40**(11), 1527-1534.

Albrecht, M, Creighton, J (1977): Anomalously intense Raman spectra of pyridine at a silver electrode. *Journal of the American Chemical,* **99**(15), 5215–5217.

Álvarez-Puebla, R, Contreras-Cáceres, R, Pastoriza-Santos, I, Pérez-Juste, J, Liz-Marzán, L (2009): Au@pNIPAM Colloids as Molecular Traps for Surface-Enhanced, Spectroscopic, Ultra-Sensitive Analysis. *Angewandte Chemie International Edition,* **48**(1), 138-143.

Álvarez-Puebla, R A, Liz-Marzán, L M (2010): SERS-Based Diagnosis and Biodetection. *Small,* **6**(5), 604-610.

Amin, F, Yushchenko, D A, Montenegro, J M, Parak, W J (2012): Integration of Organic Fluorophores in the Surface of Polymer-Coated Colloidal Nanoparticles for Sensing the Local Polarity of the Environment. *ChemPhysChem,* **13**(4), 1030-1035.

Aroca, R (2007): SERS/SERRS, the Analytical Tool. *Surface-Enhanced Vibrational Spectroscopy*. 141-184.

Bråten, T (1978): High Resolution Scanning Electron Microscopy in Biology: Artefacts Caused By the Nature and Mode of Application of the Coating Material. *Journal of Microscopy*, **113**(1), 53-59.

Cardinal, M F, Rodríguez-González, B, Alvarez-Puebla, R A, Pérez-Juste, J, Liz-Marzán, L M (2014): Modulation of Localized Surface Plasmons and SERS Response in Gold Dumbbells through Silver Coating. *The Journal of Physical Chemistry C,* **114**(23), 10417-10423.

Chen, H, Kern, E, Ziegler, C, Eychmüller, A (2009): Ultrasonically Assisted Synthesis of 3D Hierarchical Silver Microstructures. *The Journal of Physical Chemistry C,* **113**(44), 19258-19262.

de Abajo, F J G (2007): Colloquium: Light scattering by particle and hole arrays. *Reviews of Modern Physics,* **79**(4), 1267-1290.

Doering, W E, Nie, S (2003): Spectroscopic Tags Using Dye-Embedded Nanoparticles and Surface-Enhanced Raman Scattering. *Analytical Chemistry,* **75**(22), 6171-6176.

Doering, W E, Piotti, M E, Natan, M J, Freeman, R G (2007): SERS as a Foundation for Nanoscale, Optically Detected Biological Labels. *Advanced Materials,* **19**(20), 3100-3108.

Egerton, R F, Li, P, Malac, M (2004): Radiation damage in the TEM and SEM. *Micron,* **35**(6), 399-409.

Etchegoin, P G, Le Ru, E C, Meyer, M (2006): An analytic model for the optical properties of gold. *The Journal of Chemical Physics,* **125**(16), 164705.

Evans, P, Matsunaga, H, Kiguchi, M (2008): Large-scale application of nanotechnology for wood protection. *Nature Nanotechnology,* **3**(10), 577-577.

Fenniri, H, Alvarez-Puebla, R, (2007): High-throughput screening flows along. *Nature Chemical Biology,* **3**(5), 247-249.

Fernández-López, C, Mateo-Mateo, C, Álvarez-Puebla, R A, Pérez-Juste, J, Pastoriza-Santos, I, Liz-Marzán, L M (2009): Highly Controlled Silica Coating of PEG-Capped Metal Nanoparticles and Preparation of SERS-Encoded Particles. *Langmuir,* **25**(24), 13894-13899.

Fleischmann, M, Hendra, P J, McQuillan, A J (1974): Raman spectra of pyridine adsorbed at a silver electrode. *Chemical Physics Letters,* **26**(2), 163-166.

Freeman, M, McIntyre, C (2008): A comprehensive review of copper based wood preservatives. *Forest Products Journal,* **58**(11), 6-27.

Gilkey, J C, Staehelin, L A (1986): Advances in ultrarapid freezing for the preservation of cellular ultrastructure. *Journal of Electron Microscopy Technique,* **3**(2), 177-210.

Hao, F, Nehl, C L, Hafner, J H, Nordlander, P, Hafner, J H (2007): Plasmon Resonances of a Gold Nanostar. *Nano Letters,* **7**(3), 729-732.

Hrelescu, C, Sau, T K, Rogach, A L, Jäckel, F, Feldmann, J (2009): Single gold nanostars enhance Raman scattering. *Applied Physics Letters,* **94**(15), 153113.

Izumi, C M S, Moffitt, M G, Brolo, A G (2014): Statistics on Surface-Enhanced Resonance Raman Scattering from Single Nanoshells. *The Journal of Physical Chemistry C,* **115**(39), 19104-19109.

Jeanmaire, D L, van Duyne, R P (1977): Surface raman spectroelectrochemistry. *Journal of Electroanalytical Chemistry and Interfacial Electrochemistry,* **84**(1), 1-20.

Jones, R (2008): The economy of promises. *Nature Nanotechnology*, **3**(2), 65-66.

Kamel, S (2007): Nanotechnology and its applications in lignocellulosic composites, a mini review. *Express Polymer Letters*, **1**(9), 546-575.

Kneipp, K, Wang, Y, Kneipp, H, Perelman, L T, Itzkan, I, Dasari, R R, Feld, M S (1997): Single Molecule Detection Using Surface-Enhanced Raman Scattering (SERS). *Physical Review Letters*, **78**(9), 1667-1670.

Kobayashi, Y, Katakami, H, Mine, E, Nagao, D, Konno, M, Liz-Marzán, L M (2005). Silica coating of silver nanoparticles using a modified Stöber method. *Journal of Colloid and Interface Science,* **283**(2), 392-396.

Kozak, D, Kithva, P, Bax, J, Surawski, P P T, Monteiro, M J, Trau, M (2011): Development of encoded particle-polymer arrays for the accelerated screening of antifouling layers. *Chemical Communications,* **47**(34), 9687.

Kumar, P S, Pastoriza-Santos, I, Rodriguez-Gonzalez, B, Abajo, F J G, Liz-Marzan, L M (2007): High-yield synthesis and optical response of gold nanostars. *Nanotechnology,* **19**(1), 015606.

Álvarez-Puebla, R A (2012): Effects of the Excitation Wavelength on the SERS Spectrum. *J. Physical Chemistry Letters*, **3**(7), 857-866.

Leach, J, *Micronized wood preservative formulations*. United States Patent Application 20060288904.

Liz-Marzán, L M, Giersig, M, Mulvaney, P (1996): Synthesis of Nanosized Gold−Silica Core−Shell Particles. *Langmuir,* **12**(18), 4329-4335.

Ma, J, Ji, Z, Zhou, X, Zhang, Z, Xu, F (2013): Transmission Electron Microscopy, Fluorescence Microscopy, and Confocal Raman Microscopic Analysis of Ultrastructural and Compositional Heterogeneity of Cornus alba L. Wood Cell Wall. *Microscopy and Microanalysis*, **19**, 243-253.

Maurer, A, Fengel, D (1991): Electron microscopic representation of structural details in softwood cell by very thin ultramicrotome sections. *European Journal of Wood and Wood Products*, **49**(2), 53-56.

Michalet, X, Pinaud, F, Bentolila, L, Tsay, J, Doose, S (2005): Quantum dots for live cells, in vivo imaging, and diagnostics. *Science*, **307**(5709), 538-544.

Mukhopadhyay, S M (2003): Sample Preparation for Microscopic and Spectroscopic Characterization of Solid Surfaces and Films. *Sample Preparation Techniques in Analytical Chemistry*, **162**(9)377-411.

Mulvaney, P (1995): Surface Plasmon Spectroscopy of Nanosized Metal Particles. *Langmuir*, **12**(3), 788-800.

Pandey, K K, Upreti, N K, Srinivasan, V V (1998): A fluorescence spectroscopic study on wood. *Wood science and technology*, **32**(4), 309-315.

Prodan, E, Nordlander, P, Halas, N J (2003): Electronic Structure and Optical Properties of Gold Nanoshells. *Nano Letters,* **3**(10), 1411-1415.

Qian, X, Nie, S M (2008): Single-molecule and single-nanoparticle SERS: from fundamental mechanisms to biomedical applications. *Chemical Society Reviews,* **37**(5), 912.

Rodríguez-Lorenzo, L, Álvarez-Puebla, R A, Pastoriza-Santos, I, Mazzucco, S, Stéphan, O, Kociak, M, Liz-Marzán, L M, de Abajo, F J G (2009): Zeptomol Detection Through Controlled Ultrasensitive Surface-Enhanced Raman Scattering. *Journal of the American Chemical Society,* **131**(13), 4616-4618.

Rodríguez-Lorenzo, L, Álvarez-Puebla, R A, de Abajo, F J G, Liz-Marzán, L M (2014): Surface Enhanced Raman Scattering Using Star-Shaped Gold Colloidal Nanoparticles. *The Journal of Physical Chemistry C* **114**(16), 7336-7340.

Rodríguez-Lorenzo, L, Krpetic, Z, Barbosa, S, Alvarez-Puebla, R A, Liz-Marzán, L M, Prior, I A, Brust, M (2011a): Intracellular mapping with SERS-encoded gold nanostars. *Integrative Biology,* **3**(9), 922-926.

Rodríguez-Lorenzo, L, de La Rica, R, Álvarez-Puebla, R A, Liz-Marzán, L M, Stevens, M M (2012): Plasmonic nanosensors with inverse sensitivity by means of enzyme-guided crystal growth. *Nature Materials,* **11**(7), 604-607.

Rodríguez-Lorenzo, L, Romo-Herrera, J M, Pérez-Juste, J, Alvarez-Puebla, R A, Liz-Marzán, L M (2011b): Reshaping and LSPR tuning of Au nanostars in the presence of CTAB. *Journal of Materials Chemistry,* **21**(31), 11544-11549.

Stöber, W, Fink, A, Bohn, E (1968): Controlled growth of monodisperse silica spheres in the micron size range. *Journal of Colloid and Interface Science,* **26**(1), 62-69.

Weiss, S (1999): Fluorescence Spectroscopy of Single Biomolecules. *Science*, **283**(5408), 1676-1683.

Zhao, J, Dieringer, J A, Zhang, X, Schatz, G C, van Duyne, R P (2008): Wavelength-Scanned Surface-Enhanced Resonance Raman Excitation Spectroscopy. *The Journal of Physical Chemistry C*, **112**(49), 19302-19310.